

Christof Holzer,¹ Xin Gui,¹ Michael E. Harding,² Georg Kresse,³ Trygve Helgaker,^{4,5} and Wim Klopper*^{1,2,5}¹ *Institute of Physical Chemistry,
Karlsruhe Institute of Technology (KIT),
KIT Campus South, P. O. Box 6980,
D-76049 Karlsruhe, Germany*² *Institute of Nanotechnology,
Karlsruhe Institute of Technology (KIT),
KIT Campus North, P. O. Box 3640,
D-76021 Karlsruhe, Germany*³ *University of Vienna,
Faculty of Physics and Center for Computational Materials Science,
Sensengasse 8/12, A-1090 Vienna, Austria*⁴ *Hylleraas Centre for Quantum Molecular Sciences,
Department of Chemistry, University of Oslo,
P. O. Box 1033, N-0315 Oslo, Norway*⁵ *Centre for Advanced Study (CAS) at The Norwegian Academy of Science and Letters,
Drammensveien 78, N-0271 Oslo, Norway**Corresponding author, e-mail: klopper@kit.edu

A variety of approaches is presented for the computation of atomic and molecular correlation energies based on the Bethe–Salpeter equation in the framework of the adiabatic-connection fluctuation-dissipation theorem. The performance of the approaches is assessed by computing the total energies of the atoms H–Ne, the atomization energies of the HEAT set of small molecules as well as by determining the bond lengths and harmonic vibrational frequencies of the metal monoxides MO with $M = \text{Ca–Zn}$.

Keywords: Correlation energy; adiabatic connection; fluctuation–dissipation theorem; random-phase approximation; *GW* approximation, Bethe–Salpeter equation

I. INTRODUCTION

In the present work, we are concerned with the calculation of correlation energies in the framework of the adiabatic-connection fluctuation–dissipation theorem in the context of the Bethe–Salpeter equation (BSE) and its variants.

The Bethe–Salpeter equation has been used extensively in solid-state physics to calculate optical properties of solids.^{1,2} Recently, methods based on the BSE have also become popular tools for the computation of atomic and molecular electronic excitation energies. See, for example, Ref. 3 for a comprehensive review of recent BSE applications in the area of quantum chemistry.

Last year, in view of its success, the BSE approach was implemented in the TURBOMOLE program package^{4,5} by Krause and Klopper,⁶ and shortly thereafter, the performance of the BSE approach for the computation of singlet and triplet excitation energies of small molecules was carefully assessed by Gui and co-workers⁷ with respect to the quasiparticle energies used in the BSE calculations. In their *GW* computations, quasiparticle energies were computed at various levels of sophistication for all orbital levels from full spectral functions.⁷

In 2016, Maggio and Kresse used the Bethe–Salpeter equation to compute the electron-correlation energy of the homogeneous electron gas in the framework of the adiabatic-connection fluctuation–dissipation theorem.⁸

To avoid the occurrence of imaginary eigenmodes, an approximation to the BSE kernel was proposed that was referred to as “random phase approximation with screened exchange” (RPAsX).

These two approaches are just two examples of random phase-approximation (RPA) methods. A series of such methods have been proposed in recent years for the computation of electron-correlation energies of atomic and molecular systems (for a presentation of many of these variants, see Refs. 9–14), and the purpose of the present work is to assess the performance of Maggio and Kresse’s BSE and RPAsX approaches in cases where these are applied to atomic or molecular systems, for example with respect to computations of atomic total energies, atomization energies of small organic molecules, or potential curves of diatomic molecules. For this purpose, the BSE and RPAsX approaches (and many more) were implemented in the TURBOMOLE program package^{4,5} in the course of the present work, on the basis of the BSE implementation of Ref. 6 and the *GW* implementation of Ref. 7.

The present paper is organized as follows: in Section IIA, we start by recapitulating the direct random phase approximation (dRPA), where “direct” refers to the fact that exchange contributions are not taken into account. In Section IIB, we introduce exchange contributions by inserting antisymmetrized two-electron integrals into the orbital-rotation matrices when computing the two-particle density matrix, as done in Ref. 15. Mag-

g and Kresse's BSE and RPAsX approaches are obtained by inserting (static) screened exchange integrals in place of pure exchange integrals. In Section II C, we closely follow Ref. 14 for the construction of a few more approaches by inserting exchange integrals into the interaction kernel. Section II D is concerned with approaches in the framework of ring-coupled-cluster theory. Computational details needed to reproduce the results of the present work are given in Section III, and numerical results are presented in Section IV with respect to the total energies of the atoms H–Ne, the atomization energies of the HEAT (“high-accuracy extrapolated *ab initio* thermochemistry”) test set,¹⁶ and the bond lengths and harmonic vibrational frequencies of 3*d* transition-metal monoxides. Conclusions are collected in Section V.

II. THEORY

A. Direct random-phase approximation

In the direct random-phase approximation (dRPA), the correlation energy is obtained by integration over the coupling-strength parameter λ within the framework of the adiabatic connection,¹⁰

$$E_c^{\text{dRPA}} = \frac{1}{2} \int_0^1 \text{tr}(\mathbf{K}\mathbf{P}_\lambda) d\lambda, \quad (1)$$

where the interaction kernel \mathbf{K} is given by^{14,17–19}

$$\mathbf{K} = \begin{pmatrix} \mathbf{A}' & \mathbf{B} \\ \mathbf{B}^* & \mathbf{A}'^* \end{pmatrix}, \quad (2)$$

with

$$A'_{ia,jb} = v_{ia,jb} = \langle ib|aj \rangle = \int \int \varphi_i^*(\mathbf{x}_1) \varphi_b^*(\mathbf{x}_2) r_{12}^{-1} \varphi_a(\mathbf{x}_1) \varphi_j(\mathbf{x}_2) d\mathbf{x}_1 d\mathbf{x}_2, \quad (3)$$

and

$$B_{ia,jb} = v_{ia,bj} = \langle ij|ab \rangle = \int \int \varphi_i^*(\mathbf{x}_1) \varphi_j^*(\mathbf{x}_2) r_{12}^{-1} \varphi_a(\mathbf{x}_1) \varphi_b(\mathbf{x}_2) d\mathbf{x}_1 d\mathbf{x}_2. \quad (4)$$

Note that the matrix \mathbf{A}' is Hermitian while the matrix \mathbf{B} is symmetric, which makes \mathbf{K} Hermitian. Furthermore, we note that the two matrices \mathbf{A}' and \mathbf{B} are only equal when real-valued spin orbitals are used. These matrices are not equal when complex-valued spin orbitals or spinors are used, as they for example occur in quasirelativistic two-component calculations including spin–orbit effects or in calculations on atoms and molecules in finite magnetic fields.

The Hermitian matrix

$$\mathbf{P}_\lambda = \begin{pmatrix} \mathbf{Y}_\lambda \mathbf{Y}_\lambda^\dagger & \mathbf{Y}_\lambda \mathbf{X}_\lambda^\dagger \\ \mathbf{X}_\lambda \mathbf{Y}_\lambda^\dagger & \mathbf{X}_\lambda \mathbf{X}_\lambda^\dagger \end{pmatrix}^* - \begin{pmatrix} \mathbf{0} & \mathbf{0} \\ \mathbf{0} & \mathbf{1} \end{pmatrix}, \quad (5)$$

which is the correlation part of the two-particle density matrix at coupling strength λ , is obtained from solving the following non-Hermitian eigenvalue problem at coupling strength λ :

$$\begin{pmatrix} \mathbf{A}_\lambda & \mathbf{B}_\lambda \\ -\mathbf{B}_\lambda^* & -\mathbf{A}_\lambda^* \end{pmatrix} \begin{pmatrix} \mathbf{X}_\lambda & \mathbf{Y}_\lambda^* \\ \mathbf{Y}_\lambda & \mathbf{X}_\lambda^* \end{pmatrix} = \begin{pmatrix} \mathbf{X}_\lambda & \mathbf{Y}_\lambda^* \\ \mathbf{Y}_\lambda & \mathbf{X}_\lambda^* \end{pmatrix} \begin{pmatrix} \omega_\lambda & \mathbf{0} \\ \mathbf{0} & -\omega_\lambda \end{pmatrix}. \quad (6)$$

The two-particle density matrix \mathbf{P}_λ is related to the polarization propagator $\mathbf{\Pi}_\lambda$ via the fluctuation–dissipation theorem,

$$\mathbf{P}_\lambda = \frac{1}{2\pi i} \int_{-\infty}^{\infty} e^{i\omega\tau} [\mathbf{\Pi}_\lambda(\omega) - \mathbf{\Pi}_0(\omega)] d\omega. \quad (7)$$

In Eq. (6), the eigenvalues are (approximate) excitation and de-excitation energies of the atom or molecule, and the matrices \mathbf{A}_λ and \mathbf{B}_λ are given by

$$(A_\lambda)_{ia,jb} = \Delta_{ia,jb} + \lambda A'_{ia,jb}, \quad (8)$$

$$(B_\lambda)_{ia,jb} = \lambda B_{ia,jb}, \quad (9)$$

where $\Delta_{ia,jb} = (\varepsilon_a - \varepsilon_i) \delta_{ij} \delta_{ab}$. Here, the ε_p are orbital or quasiparticle energies of the canonical spin orbitals φ_p . We denote occupied spin orbitals by i, j, k, \dots and virtual spin orbitals by a, b, c, \dots .

The eigenvectors of Eq. (6) are normalized to

$$\mathbf{X}_\lambda^\dagger \mathbf{X}_\lambda - \mathbf{Y}_\lambda^\dagger \mathbf{Y}_\lambda = \mathbf{1}, \quad (10)$$

and the working equation for the dRPA integrand reads

$$\text{tr}(\mathbf{K}\mathbf{P}_\lambda) = \text{tr}(\mathbf{X}_\lambda^\dagger \mathbf{B} \mathbf{Y}_\lambda + \mathbf{Y}_\lambda^\dagger \mathbf{B}^* \mathbf{X}_\lambda) + \text{tr}(\mathbf{X}_\lambda^\dagger \mathbf{A}' \mathbf{X}_\lambda + \mathbf{Y}_\lambda^\dagger \mathbf{A}'^* \mathbf{Y}_\lambda) - \text{tr}(\mathbf{A}'). \quad (11)$$

This trace is real-valued since the matrices \mathbf{K} and \mathbf{P}_λ are Hermitian.

B. Exchange in the polarization propagator

Next we introduce exchange contributions by defining matrices with “antisymmetrized” two-electron integrals. As in Ref. 15, we indicate these matrices by an overbar,

$$(\bar{A}_\lambda)_{ia,jb} = \Delta_{ia,jb} + \lambda v_{ia,jb} - \lambda v_{ij,ab}, \quad (12)$$

$$(\bar{B}_\lambda)_{ia,jb} = \lambda v_{ia,bj} - \lambda v_{ib,aj}. \quad (13)$$

Based on these matrices, the RPA *exchange* (RPax) correlation energy is given by^{20,21}

$$E_c^{\text{RPax}} = \frac{1}{2} \int_0^1 \text{tr}(\mathbf{K}\bar{\mathbf{P}}_\lambda) d\lambda, \quad (14)$$

where $\bar{\mathbf{P}}_\lambda$ is obtained from solving Eq. (6) using \bar{A}_λ and \bar{B}_λ in place of A_λ and B_λ .

The Bethe–Salpeter correlation energy as defined in Ref. 8 is given by an expression very similar to Eq. (14), the only difference being that the exchange terms in Eqs. (12) and (13) are replaced by their static screened counterparts. Correspondingly, the Bethe–Salpeter correlation energy is obtained from

$$E_c^{\text{BSE}} = \frac{1}{2} \int_0^1 \text{tr} \left(\mathbf{K} \bar{\mathbf{P}}_\lambda \right) d\lambda, \quad (15)$$

where $\bar{\mathbf{P}}_\lambda$ is obtained from solving Eq. (6) using \bar{A}_λ and \bar{B}_λ in place of A_λ and B_λ ,

$$\left(\bar{A}_\lambda \right)_{ia,jb} = \Delta_{ia,jb} + \lambda v_{ia,jb} - \lambda w_{ij,ab}, \quad (16)$$

$$\left(\bar{B}_\lambda \right)_{ia,jb} = \lambda v_{ia,bj} - \lambda w_{ib,aj}. \quad (17)$$

In Eqs. (16) and (17), w refers to integrals over the static screened interaction. As in Ref. 6, these integrals are computed in the resolution-of-the-identity (RI) approximation,

$$w_{pq,rs} = \sum_{PQ} R_{pq,P} (\epsilon^{-1})_{PQ} R_{Q,rs}, \quad (18)$$

with

$$\epsilon_{PQ} = \delta_{PQ} - 2\Re \sum_{kc} \frac{R_{P,kc} R_{kc,Q}}{\epsilon_k - \epsilon_c}, \quad (19)$$

where \Re denotes the real part. Here, the indices p, q, r, \dots refer to arbitrary spin orbitals while the indices P, Q, R, \dots refer to functions of the (real-valued) auxiliary basis set. The integrals R are the usual three-index intermediate quantities that occur in methods based on the RI approximation (see Ref. 6 for details).

In Ref. 8, the RPAsX approximation (random-phase approximation with screened exchange) was proposed to resolve problems due to instabilities originating from particle–hole diagrams. In this RPAsX approximation, the term $-\lambda w_{ij,ab}$ in Eq. (16) is omitted.

Furthermore, we note that instead of multiplying the final integral w with the coupling-strength parameter λ , as done in Ref. 8, the concept of coupling-strength integration implies that at coupling strength λ , the two-electron integrals need to be scaled by λ . After some straightforward manipulation, one can show that the screened interaction w at coupling strength λ is given by the following equations:

$$(\epsilon_\lambda)_{PQ} = \delta_{PQ} - 2\lambda \Re \sum_{kc} \frac{R_{P,kc} R_{kc,Q}}{\epsilon_k - \epsilon_c}, \quad (20)$$

$$w_{pq,rs}^\lambda = \sum_{PQ} R_{pq,P} (\epsilon_\lambda^{-1})_{PQ} R_{Q,rs}, \quad (21)$$

and

$$\left(\tilde{A}_\lambda \right)_{ia,jb} = \Delta_{ia,jb} + \lambda v_{ia,jb} - \lambda w_{ij,ab}^\lambda, \quad (22)$$

$$\left(\tilde{B}_\lambda \right)_{ia,jb} = \lambda v_{ia,bj} - \lambda w_{ib,aj}^\lambda. \quad (23)$$

The corresponding correlation energy, which we denote as *extended* Bethe–Salpeter (XBS) correlation energy, is then given by

$$E_c^{\text{XBS}} = \frac{1}{2} \int_0^1 \text{tr} \left(\mathbf{K} \tilde{\mathbf{P}}_\lambda \right) d\lambda. \quad (24)$$

Equations (20)–(24) were straightforward to implement in the TURBOMOLE program package. The previously applied equations (18)–(19) are obviously an approximation, which is only exact at small λ .

We note that the corresponding XBSsX correlation energy is obtained by omitting the term $-\lambda w_{ij,ab}^\lambda$ in Eq. (22).

C. Exchange in the interaction kernel

More energy expressions can be generated by replacing the matrix \mathbf{K} in Eqs. (1), (14), (15), or (24) by its “antisymmetrized” counterpart $\tilde{\mathbf{K}}$. For example, by making this replacement in Eq. (1), the dRPA-II correlation energy of Ángyán *et al.* is obtained,^{14,17} which is closely related to the adiabatic-connection second-order screened exchange (AC-SOSEX) correlation energy,

$$E_c^{\text{dRPA-II}} = \frac{1}{2} \int_0^1 \text{tr} \left(\tilde{\mathbf{K}} \mathbf{P}_\lambda \right) d\lambda. \quad (25)$$

The AC-SOSEX correlation energy refers to the dRPA-IIa approximation defined by equation 59 of Ref. 14.

In the spirit of Eq. (25), it seems also worthwhile to investigate the corresponding expression using the interaction kernel $\tilde{\tilde{\mathbf{K}}} = \tilde{\mathbf{K}}$, where the antisymmetric (exchange-like) contribution is evaluated with the static screened exchange w at full coupling ($\lambda = 1$) instead of v . The correlation energy is then defined as

$$E_c^{\text{IOSEX}} = \frac{1}{2} \int_0^1 \text{tr} \left(\tilde{\tilde{\mathbf{K}}} \mathbf{P}_\lambda \right) d\lambda. \quad (26)$$

We denote this new approach as IOSEX (infinite-order screened exchange) approach.

Furthermore, we have also investigated correlation-energy expressions in which only the matrix \mathbf{B} is inserted into Eq. (11) in antisymmetrized (and possibly screened) form. This resembles the “sX” approximation of Ref. 8 and we therefore denote the corresponding approaches by the ending “sX”. For example, we define the dRPA-IIsX

correlation energy as

$$E_c^{\text{dRPA-II}sX} = \frac{1}{2} \int_0^1 \text{tr}(\bar{\mathbf{K}}_{sX} \mathbf{P}_\lambda) d\lambda, \quad (27)$$

with

$$\bar{\mathbf{K}}_{sX} = \begin{pmatrix} \mathbf{A}' & \bar{\mathbf{B}} \\ \bar{\mathbf{B}}^* & \mathbf{A}'^* \end{pmatrix}. \quad (28)$$

The IOSEXsX correlation energy is defined analogously in terms of a matrix $\bar{\mathbf{K}}_{sX}$ that contains $\bar{\mathbf{B}}$.

D. Ring-coupled-cluster theory

At this point, we note that it is also possible to define the second-order screened exchange correlation energy in the framework of the direct ring-coupled-cluster-doubles (drCCD) approach, which is equivalent to the dRPA method. We refer to this drCCD-based variant as coupled-cluster second-order screened exchange (CC-SOSEX) correlation energy.²² It is defined as

$$E_c^{\text{CC-SOSEX}} = \frac{1}{2} \text{tr}(\bar{\mathbf{B}} \mathbf{Y}_1 \mathbf{X}_1^{-1}). \quad (29)$$

Analogously, we define the coupled-cluster infinite-order screened exchange (CC-IOSEX) correlation energy as

$$E_c^{\text{CC-IOSEX}} = \frac{1}{2} \text{tr}(\tilde{\mathbf{B}} \mathbf{Y}_1 \mathbf{X}_1^{-1}). \quad (30)$$

E. Overview over all methods

An overview over the abovementioned methods is given in Table I. Here and in the following, we use blackboard bold characters to represent any of the matrices given in the previous sections. With respect to the integrand $\text{tr}(\mathbb{K} \mathbf{P}_\lambda)$ entering the coupling-strength integration, one needs to ask the following questions: first, how does one construct the matrices \mathbf{A}' and \mathbb{B} to set up \mathbb{K} , second, how does one construct the matrices \mathbf{A}'_λ and \mathbb{B}_λ that are used to build \mathbb{P}_λ , and third, whether to use Kohn–Sham orbital energies or *GW* quasiparticle energies. For all methods without a prime summarized in Table I, the screened exchange w in the \mathbf{A}' and \mathbb{B} matrices for the interaction kernel \mathbb{K} and in the \mathbf{A}'_λ and \mathbb{B}_λ matrices for the polarization propagator are calculated using *GW* quasiparticle energies. A prime is attached to the method's acronym if Kohn–Sham orbital energies are used for the diagonal matrix Δ in place of *GW* quasiparticle energies. When Kohn–Sham orbital energies are used everywhere, that is, also for the screened exchange w (and w^λ), then we attach a double prime to the method's acronym (not shown in Table I).

TABLE I. Overview of various models, using either orbital energies (OE) or quasiparticle energies (QP) for Δ . Given is the exchange-like contribution to the respective matrix.

Method ^a	\mathbb{K}		Δ	\mathbb{P}_λ	
	\mathbf{A}'	\mathbb{B}		\mathbf{A}'_λ	\mathbb{B}_λ
CC-SOSEX	$-^b$	v	OE	0	0
CC-IOSEX	$-^b$	w	QP	0	0
CC-IOSEX'	$-^b$	w	OE	0	0
dRPA ^c	0	0	OE	0	0
dRPA-II	v	v	OE	0	0
dRPA-IIsX	0	v	OE	0	0
IOSEX	w	w	QP	0	0
IOSEX'	w	w	OE	0	0
IOSEXsX	0	w	QP	0	0
IOSEXsX'	0	w	OE	0	0
BSE	0	0	QP	w	w
BSE'	0	0	OE	w	w
RPAsX	0	0	QP	0	w
RPAsX'	0	0	OE	0	w
XBS	0	0	QP	w^λ	w^λ
XBS'	0	0	OE	w^λ	w^λ
XBSsX	0	0	QP	0	w^λ
XBSsX'	0	0	OE	0	w^λ
RPax ^d	0	0	OE	v	v
RPax-II ^e	v	v	OE	v	v

a) The prime indicates that quasiparticle energies are used for w but not for Δ .

b) Energy computed from drCCD amplitudes and \mathbb{B} .

c) dRPA \equiv dRPA-I.

d) RPax \equiv RPax-I.

e) See Ref. 14.

A few comments are in place here. First, we have grouped Table I into different categories. The first three lines correspond to time-ordered perturbation theory as realized in the coupled-cluster approach. The next seven methods use the direct RPA to determine the polarization propagator but contract over different (possibly antisymmetrized) interaction kernels. If the polarization propagator is calculated in the direct RPA, antisymmetrization of the interaction kernel \mathbb{K} seems advantageous. Inspired by the observation by Maggio and Kresse⁸ that instabilities can be avoided by using only antisymmetrized \mathbb{B} kernels, we have investigated this approximation for the interaction kernel \mathbb{K} as well (...sX methods). The next nine methods apply direct RPA-like kernels for the interaction \mathbb{K} but calculate the polarization propagator either in the full random-phase approximation (RPax method) or by using the full Bethe–Salpeter polarization propagator with antisymmetrized \mathbf{A}'_λ and \mathbb{B}_λ matrices. The final method (RPax-II) uses

antisymmetrized matrices in both the polarization propagator and the interaction kernel.

As to what kind of combinations are expected to be useful, the following issues are important:

Common experience tells that orbitals and one-electron energies obtained from density-functional theory (DFT) combined with the dRPA yield reasonable polarizabilities (for instance, DFT static dielectric constants, C_6 coefficients and symmetry-adapted perturbation theory using DFT polarizabilities are often remarkably accurate).²³ Combined with a dRPA kernel, the correlation energies are too negative, but that can be alleviated by contracting over an antisymmetrized interaction kernel. Combining dRPA polarizabilities with antisymmetrized interaction kernels restores the direct and exchange diagram in second order.

If quasiparticle energies are used to calculate the independent-particle propagator, one needs to include the antisymmetric terms in the A'_λ and B_λ matrices of the Bethe–Salpeter equation to obtain quantitatively reliable excitation spectra and polarizabilities. Specifically, combining quasiparticle energies with the dRPA yields much too small polarizabilities as shown in Ref. 24. To obtain accurate results, the inclusion of w (or w^λ) in A'_λ is particularly important, as this term introduces excitonic effects via the particle-hole ladder diagrams. However, including screened (w or w^λ) unscreened (v) exchange integrals in the A'_λ matrix often introduces instabilities causing negative eigenvalues in the excitation spectrum (cf. Ref. 8). As discussed in the results section, these methods turn out to be unstable for most systems;

Inclusion of the exchange diagrams only in the B_λ matrix of the polarization propagator resolves the instability issues. Fundamentally, however, it is unclear whether this approach should be combined with DFT orbital energies or GW quasiparticle energies. Since excitonic effects are neglected (no exchange diagrams in the A'_λ matrix), it seems reasonable to test this approach with both DFT orbital energies or GW quasiparticle energies, with DFT orbital energies possibly having a slight advantage.

III. COMPUTATIONAL DETAILS

All adiabatic-connection correlation-energy calculations were performed with the TURBOMOLE program package using the modules DSCF (for Kohn–Sham calculations), ESCF (for the GW quasiparticle energies and Bethe–Salpeter correlation energies), and RIRPA (for dRPA and AXK). The CFOUR program (*Coupled-Cluster techniques for Computational Chemistry*)²⁵ was used for the coupled-cluster calculations on the transition-metal monoxides at the coupled-cluster singles-and-doubles level with perturbative triples, CCSD(T).^{26,27}

A. Atomic total energies and HEAT test set

The calculations were performed in the aug-cc-pwCVXZ (aug-cc-pVXZ for H) basis sets of Peterson and Dunning,^{28–30} with $X = T, Q$ and 5. When using the ESCF module, the “MP2-fitting” basis set of Hättig was used as auxiliary basis set for the RI approximation (CBAS in TURBOMOLE jargon).³¹ When using the RIRPA module, Weigend’s universal “Coulomb-fitting” basis was used for the RI approximation (JBAS in TURBOMOLE jargon).³²

The complete-basis-set (CBS) total and atomization energies were obtained by fitting the function $E_{\text{ref}}(\infty) + \alpha \exp(-\beta X)$ to the Kohn–Sham determinant expectation values obtained in aug-cc-pVXZ basis sets²⁸ with $X = Q, 5$ and 6 ($X = T, Q$ and 5 for Li and Be) and by fitting the function $E_c(\infty) + \gamma X^{-3}$ to the correlation energies obtained in aug-cc-pwCVXZ (aug-cc-pVXZ for H) basis sets with $X = Q$ and 5.^{33,34} We refer to this extrapolation as Q56/Q5 extrapolation.

Quasiparticle energies were computed at the evGW level³⁵ with TURBOMOLE’s ESCF module using the implementation of Ref. 7. In these calculations, the relevant TURBOMOLE parameters were set to `eta = 0.05` and `rpaconv = 5`. Numerical integration over coupling strength was done using a Gauß–Legendre quadrature using 32 points or more. The evGW level was chosen because it was found to outperform the (linearized) G_0W_0 scheme with respect to electronic excitation energies, yielding an accuracy similar to that of the computationally more involved quasiparticle self-consistent approach (qsGW).⁷

The functionals TPSS³⁶ and TPSSh^{37,38} were employed in the Kohn–Sham calculations, using the TURBOMOLE parameters `gridsize = 5`, `scfconv = 10`, and `denconv = 1d-9`.

In Ref. 39, Bates and Furche argue that the reference determinant for RPA correlation-energy calculations is most appropriately generated from a (non-hybrid) semi-local DFT calculation. They recommend the TPSS functional, but we decided to also test the hybrid functional TPSSh. At this point, a comprehensive study of functionals must be postponed into the future.

B. Transition-metal monoxides

The computations on the 3d transition-metal monoxides were all performed in the def2-QZVPP basis set of Weigend, Ahlrichs and Furche.⁴⁰ As for the atomic total energies and atomization energies, the “MP2-fitting” basis set of Hättig was used as CBAS auxiliary basis set for the RI approximation³¹ while for computations with the RIRPA module, Weigend’s universal “Coulomb-fitting” JBAS basis was used.³² Quasiparticle energies were computed at the evGW level³⁵ using the parameters `eta = 0.05` and `rpaconv = 5`. The underlying Kohn–Sham calculations were performed with the func-

tionals TPSS³⁶ and TPSSh^{37,38} using the TURBOMOLE parameters `gridsize = 5`, `scfconv = 9`, and `denconv = 10`. Calculations were performed for the same electronic states as given in Table VI of Ref. 41, and for each system the equilibrium geometry and harmonic vibrational frequency were determined by fitting a 6th-degree polynomial to seven points about the minimum of the potential-energy curve (of the method of interest), using an equidistant spacing of $0.02 a_0$. Numerical integration over coupling strength was done using a Gauß-Legendre quadrature using 32 points or more.

IV. RESULTS AND DISCUSSION

In this section, we will discuss results that were obtained using Kohn–Sham orbitals obtained from DFT calculations with the TPSS functional.³⁶ All of these calculations have been repeated with TPSSh orbitals, but the results obtained with this hybrid functional have been moved to the Supplemental Information. The results do not depend too much on the Kohn–Sham orbitals, and it seems appropriate to focus on the TPSS results in the main text.

In the following, we will discuss the results obtained for atomic total energies, atomization energies, bond lengths, and harmonic vibrational frequencies.

Note that we do not report results of all methods mentioned in Section II because we encountered instabilities (matrices that were not positive definite) on many occasions when applying the RPax, RPax-II, BSE, BSE', XBS and XBS' methods. Thus, these methods do not occur in the tables with results. Note that the methods plagued by instabilities have in common that the matrix A' of Table I contains exchange contributions.

A. Atomic total energies

Table II shows results for the total energies of the atoms H–Ne. Computed energies are compared with the estimates for the exact nonrelativistic total energies of Davidson and co-workers.⁴² In wave function theory, the post-Hartree–Fock correlation energy is added to the Hartree–Fock energy (Hamiltonian expectation value obtained with the Hartree-Fock determinant) to obtain the total electronic energy. In the framework of the adiabatic connection, however, the correlation energy is added to the Hamiltonian expectation value computed with the Kohn–Sham determinant. Such an adiabatic-connection correlation energy can therefore not directly be compared with a post-Hartree–Fock correlation energy. Thus, we decided to extrapolate both the expectation values and the correlation energies to the limit of a complete basis, such that for each system, we can compare the sum of the two extrapolated energies with the highly accurate total electronic energy of Ref. 42.

The dRPA model yields only very poor total energies for the atoms H–Ne. Also the Bethe–Salpeter based methods using orbital energies only (instead of quasiparticle energies) do not perform very well (methods RPAsX'–IOSEXsX'). The virtually identical results for AC-SOSEX and CC-SOSEX have been observed for many systems in several studies. dRPA-II_sX is also very close, and a diagrammatic analysis shows that all three include identical diagrams up to second order in the Coulomb interaction. In third order, subtle differences exist, where AC-SOSEX includes improper diagrams. It is somewhat remarkable that the differences between CC-SOSEX/AC-SOSEX and RPAsX/XBSsX/CC-IOSEX are also small, although the latter three methods calculate the polarization propagators using GW quasiparticle energies instead of Kohn–Sham orbital energies. There is no obvious reason for this good agreement. On the other hand, the good agreement within the group RPAsX/XBSsX/CC-IOSEX is expected, since these methods use the same one-electron energies and include a very similar set of diagrams (they are again identical up to second order in the Coulomb interaction).

Replacing the quasiparticle energies by orbital energies in the diagonal matrix Δ increases the magnitude of the correlation energies consistently by about 25–35 mE_h for the atoms B–Ne. This is in line with our expectations: the one-electron gaps are smaller using orbital energies than quasiparticle energies, so fluctuations and correlation energies increase in magnitude. XBSsX' and IOSEXsX' are particularly close, and a diagrammatic analysis shows that they sum the same set of diagrams up to third order in the Coulomb interaction (in fourth order, the XBSsX' approach includes diagrams with two \mathbb{B} 's that are missing in IOSEXsX'). A more detailed diagrammatic analysis is postponed to future studies, though.

The differences between the other methods are only minor, and some of the new methods perform roughly as well as the approximate-exchange-kernel (AXK) method of Bates and Furche.³⁹

B. HEAT test set

In real-world applications of electronic-structure approaches to chemical problems of interest, energy differences are more important than total energies. In 2008, Harding *et al.*¹⁶ published accurate values for the non-relativistic electronic atomization energies for a series of small molecules using the “highly accurate extrapolated thermochemistry” (HEAT) protocol, and in Table III, we compare the results of our calculations with these HEAT reference values. Both our values and the HEAT values have been extrapolated to the complete-basis-set (CBS) limit. Deviations from the HEAT values obtained in finite basis sets are also reported. Figure 1 visualizes the deviations from the HEAT reference values for

TABLE I. Errors in the total energies (in mE_h) of the atoms H–Ne. Computed using the TPSS functional and extrapolated to the basis-set limit (Q56/Q5 extrapolation).

Method ^a	H	He	Li	Be	B	C	N	O	F	Ne
Reference ^b	−500.00	−2903.7	−7478.1	−14667	−24654	−37845	−54589	−75067	−99734	−128939
TPSS	0	−6	−10	−4	−15	−22	−27	−43	−46	−42
TPSS orbital energies										
dRPA ^c	−20	−40	−65	−81	−105	−129	−145	−169	−189	−199
AXK ^c	−2	−4	−9	−11	−10	−9	−5	−6	−6	−2
CC-SOSEX	0	1	1	6	11	13	14	17	20	22
AC-SOSEX	0	1	1	6	11	14	14	18	21	23
dRPA-II	−3	−6	−16	−27	−30	−38	−17	−28	−40	−14
dRPA-II _s X	1	3	5	14	21	25	22	28	33	34
RPAsX''	−4	−10	−18	−25	−29	−33	−27	−35	−40	−31
XBSsX''	−3	−7	−14	−18	−20	−23	−17	−23	−26	−18
CC-IOSEX''	−4	−9	−17	−23	−27	−31	−24	−32	−37	−27
IOSEX''	−7	−16	−33	−55	−63	−73	−48	−67	−81	−54
IOSEXsX''	−3	−8	−15	−20	−23	−25	−19	−26	−29	−20
evGW quasiparticle energies										
RPAsX	−2	−1	−5	8	8	7	6	8	10	12
RPAsX'	−3	−8	−13	−18	−19	−21	−20	−25	−28	−26
XBSsX	−1	1	−2	12	14	14	13	16	20	22
XBSsX'	−2	−6	−9	−12	−11	−12	−12	−14	−16	−14
CC-IOSEX	−2	0	−4	9	10	9	8	10	12	15
CC-IOSEX'	−3	−7	−12	−16	−17	−18	−18	−22	−24	−22
IOSEXsX'	−2	−6	−9	−10	−10	−11	−12	−14	−15	−15

a) One prime indicates that orbital energies are used for Δ ; a double prime indicates that orbital energies are not only used for Δ but also for w (or w^λ).

b) From Ref. 42.

c) Computed with the RIRPA module.

a few selected methods in terms of normalized Gaussian distributions. The HEAT test set comprises the 26 molecules N_2 , H_2 , F_2 , CO , O_2 , C_2H_2 , CCH , CF , CH_2 , CH , CH_3 , CN , CO_2 , H_2O_2 , H_2O , HCN , HCO , HF , HNO , HO_2 , NH_2 , NH_3 , NH , NO , OF , and OH . For molecules of this size, a mean absolute error of 31.2 kJ mol^{-1} in the atomization energies as obtained at the dRPA level is unacceptable (the standard deviation σ of the error distribution amounts to 21.9 kJ mol^{-1} , see Figure 1). This is much improved by the AXK method of Bates and Furche,³⁹ which shows a mean absolute error of 18.4 kJ mol^{-1} ($\sigma = 12.7 \text{ kJ mol}^{-1}$).

The SOSEX variants AC-SOSEX, CC-SOSEX, dRPA-II and dRPA-II_sX all yield results of poorer quality than dRPA and thus are no improvement. Very promising, however, are the methods RPAsX', XBSsX', CC-IOSEX' and IOSEXsX'. It appears that it is advantageous to use quasiparticle energies only for the screened interaction w (and/or w^λ), not for the energy differences of the matrix Δ . Since all of these methods neglect the particle-hole ladder diagrams in the A'_λ matrix, the use

of quasiparticle energies in the polarization propagator would yield too small polarizabilities and fluctuations. Using the Kohn–Sham orbital energies rectifies this problem. All of this also applies to the results obtained with the TPSSh functional (see Table S2 in the Supplemental Information). Of the above mentioned methods, the CC-IOSEX' method is particularly promising. Building the matrices \mathbf{X}_1 and \mathbf{Y}_1 is relatively straightforward and not hampered by instabilities (it is done at the dRPA level). Furthermore, no numerical integration over the coupling strength is involved (see Eq. 30).

C. Transition-metal monoxides

In view of the success of the CC-IOSEX' approach, we found it interesting to see whether the method would also perform well on a quite different set of molecules such as the $3d$ transition-metal monoxides MO with $M=Ca$ – Zn . The results of the corresponding calculations are presented and discussed in the present section.

TABLE II. Mean absolute error (in kJ mol^{-1}) with respect to the non-relativistic, electronic atomization energies of the HEAT test set. Computed using the TPSS functional.

Method	ACVTZ	ACVQZ	ACV5Z	CBS ^a
TPSS	15.1	15.5	15.6	15.6
TPSS orbital energies				
dRPA ^b	55.2	41.1	36.4	31.2
AXK ^b	46.2	30.2	24.6	18.4
CC-SOSEX	61.0	45.7	40.5	34.8
AC-SOSEX	61.1	45.8	40.6	34.9
dRPA-II	77.6	61.5	56.2	51.8
dRPA-II _s X	75.4	60.2	55.0	49.5
RPAsX''	37.5	22.3	18.5	15.9
XBSsX''	37.1	22.0	16.9	13.6
CC-IOSEX''	37.8	22.8	18.6	15.6
IOSEX''	56.6	48.8	47.1	45.4
IOSEXsX''	40.9	25.9	20.7	16.5
evGW quasiparticle energies				
RPAsX	57.6	41.0	34.7	27.8
RPAsX'	23.5	8.1	5.3	5.8
XBSsX	62.7	46.2	40.0	33.1
XBSsX'	27.7	12.3	7.1	4.0
CC-IOSEX	59.3	42.8	36.6	29.8
CC-IOSEX'	24.1	8.7	4.8	4.7
IOSEX	41.5	24.8	18.6	11.9
IOSEX'	43.2	36.1	34.5	32.9
IOSEXsX	97.1	80.4	73.9	66.9
IOSEXsX'	26.7	11.3	6.2	3.2

a) Q56/Q5 extrapolation.

b) Computed with the RIRPA module.

The 3d transition-metal monoxides have been investigated by Furche and Perdew as well as by Bates and Furche to test the TPSS functional and the AXK approach, respectively.^{39,41} As in Ref. 39, we use the def2-QZVPP basis set and compare the computed results (equilibrium bond lengths and harmonic vibrational frequencies) with experimental data. Of course, a comparison of non-relativistic, pure electronic-structure results obtained in a finite basis set of atomic orbitals with experimental results is somewhat troublesome, but we can compare our results also with those that are obtained at the Kohn–Sham, dRPA, AXK and CCSD(T) levels.

Considering the equilibrium bond length r_e , the mean error and mean absolute error of the set of 11 monoxides amount to -0.5 and 0.7 pm, respectively, at the Kohn–Sham TPSS/def2-QZVPP level (see Table IV). This is remarkably accurate, in particular in comparison with the dRPA and AXK levels, which display mean absolute errors of 1.2 and 0.8 pm, respectively (the mean errors are 0.7 and 0.0 pm, respectively). The dRPA and AXK

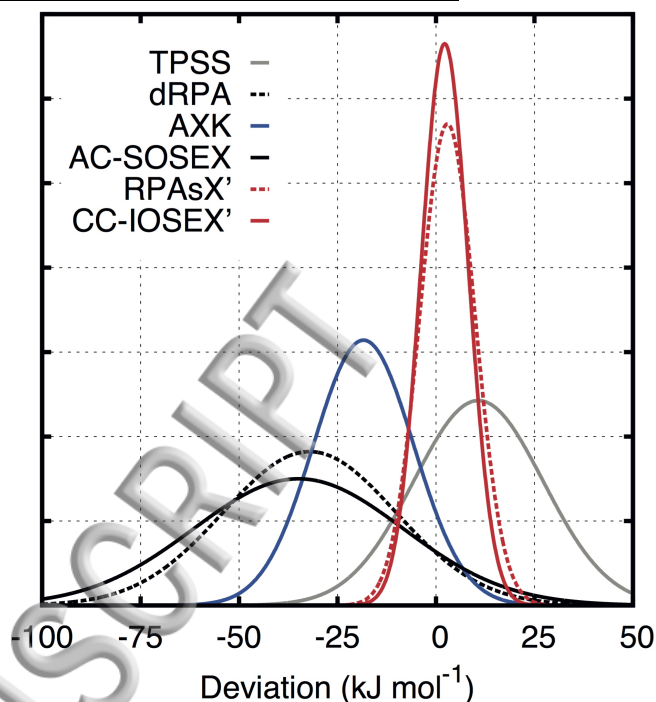


FIG. 1. Normalized Gaussian distributions of deviations from the HEAT benchmark values.

approaches do not seem to improve the underlying Kohn–Sham results.

This behavior of the TPSS, dRPA and AXK methods is corroborated by the results obtained for the harmonic vibrational frequencies ω_e (see Table V). Whereas the mean absolute error amounts to 25 cm^{-1} at the TPSS/def2-QZVPP level, these errors are 43 and 33 cm^{-1} at the dRPA and AXK levels, respectively. Also the SOSEX variants are no improvement over Kohn–Sham theory. For the bond lengths, we find mean absolute errors of 3.1 , 3.3 , 1.9 and 5.8 pm, respectively, for the methods CC-SOSEX, AC-SOSEX, dRPA-II and dRPA-II_sX. For the harmonic vibrational frequencies, the respective mean absolute errors are 97 , 103 , 52 and 180 cm^{-1} .

With respect to harmonic vibrational frequencies of individual systems, the differences between results obtained with TPSS or TPSSh orbitals seem somewhat more pronounced than for the equilibrium distances, but the corresponding mean absolute errors show a comparable order of magnitude for the TPSS- and TPSSh-based results.

Unfortunately, it is difficult to identify clear trends or approaches that perform clearly better than others. With respect to the atomization energies of the HEAT test set, the methods RPAsX', XBSsX', CC-IOSEX' and IOSEXsX' look promising, and indeed, these methods also perform (reasonably) well for the transition-metal monoxides. With respect to the bond lengths, the mean

TABLE V. Errors in the equilibrium bond lengths (r_e in pm) of transition-metal monoxides. Computed in the def2-QZVPP basis set Hartree–Fock reference for UHF-CCSD(T), TPSS reference elsewhere.

Method	CaO	ScO	TiO	VO	CrO	MnO	FeO	CoO	NiO	CuO	ZnO	MAE ^a
Expt. ^b	182.2	166.8	162.0	158.9	161.5	164.6	161.6	162.9	162.7	172.4	171.9 ^c	
CCSD(T) ^d	0.7	0.4	-0.3	-1.5	0.1	-0.3	-1.2	-2.8	-0.1	2.6	-1.2	1.0
TPSS	-1.0	0.0	1.1	0.1	-0.1	-1.7	-1.1	-0.4	0.2	-0.2	-2.0	0.7
TPSS orbital energies												
dRPA ^e	0.0	1.2	2.0	0.9	1.9	-0.7	0.3	2.8	1.2	-0.2	-2.1	1.2
AXK ^e	-0.2	-0.1	0.6	-0.9	0.2	-1.1	-0.7	0.6	-1.2	2.6	0.3	0.8
CC-SOSEX	-3.0	-2.1	-1.4	-3.0	-2.5	-2.7	-3.2	-2.5	-5.6	6.2	-1.9	3.1
AC-SOSEX	-3.1	-2.1	-1.5	-3.1	-2.8	-2.8	-3.3	-2.7	-6.0	7.0	-1.7	3.3
dRPA-II	1.5	2.1	2.5	1.6	-0.5	-0.1	2.0	-5.0	0.2	3.6	... ^f	1.9
dRPA-II _s X	-5.6	-4.0	-3.4	-5.2	-5.2	-4.9	-5.8	-4.7	-9.8	11.4	-4.1	5.8
RPAsX''	2.7	2.1	2.9	2.0	2.3	1.1	2.1	2.1	3.6	0.5	1.6	2.1
XBSsX''	2.4	1.8	2.6	1.7	2.0	1.0	1.9	1.7	3.3	0.9	1.4	1.9
CC-IOSEX''	2.8	2.2	2.9	2.1	2.3	1.2	2.2	2.2	3.8	0.6	1.7	2.2
IOSEXsX''	2.4	1.8	2.6	1.7	2.0	1.0	1.9	1.8	3.2	1.0	1.7	1.9
evGW quasiparticle energies												
RPAsX	0.6	-2.1	-1.4	-2.0	-0.8	-2.2	-1.9	-0.9	-1.4	1.3	-2.8	1.6
RPAsX'	1.6	0.9	1.7	0.6	1.1	0.0	0.4	1.0	0.9	0.5	-0.4	0.8
XBSsX	0.3	-2.3	-1.6	-2.2	-1.0	-2.3	-2.1	-1.4	-1.7	1.7	-2.9	1.8
XBSsX'	1.0	0.4	1.2	0.0	0.5	-0.4	-0.1	0.3	-0.3	1.1	-0.7	0.5
CC-IOSEX	0.6	-2.1	-1.4	-2.0	-0.8	-2.2	-1.9	-0.9	-1.4	1.4	-2.8	1.6
CC-IOSEX'	1.7	0.9	1.7	0.6	1.1	0.0	0.5	1.1	1.0	0.7	-0.4	0.9
IOSEXsX'	0.7	0.1	1.0	-0.2	0.2	-0.7	-0.5	0.1	-0.8	1.4	-1.2	0.6

a) Mean absolute error.

b) For details on experimental data, cf. Ref. 41.

c) CCSD(T) result from Ref. 43.

d) Frozen-core (M: $1s2s2p$, O: $1s$) UHF-CCSD(T)/def2-QZVPP computations with CFOUR.

e) Computed with the RIRPA module.

f) Computation failed.

absolute errors are 0.8, 0.5, 0.9 and 0.6 pm, respectively. This is roughly the same quality as obtained in the TPSS and AXK calculations. A similar conclusion can be drawn from the harmonic-vibrational-frequency results, and in view of the above, we conclude that the CC-IOSEX' approach remains a good candidate for the accurate and cost-efficient computation of correlation energies in the framework of the adiabatic-connection fluctuation–dissipation theorem.

V. CONCLUSIONS

We have implemented (in the TURBOMOLE program package) a number of methods based on the Bethe–Salpeter equation for the computation of correlation energies in the framework of the adiabatic-connection fluctuation–dissipation theorem. Inclusion of (screened)

exchange contributions when constructing the matrices \mathbb{P}_λ (see Table I) often leads to instabilities. The corresponding methods were not applicable. More useful methods were obtained when invoking the direct random-phase approximation (dRPA) when constructing \mathbb{P}_λ . Then, (screened) exchange contributions can be accounted for in the matrix \mathbb{K} (see Table I). The performance of the corresponding methods has been assessed and in particular the CC-IOSEX' approach seemed very promising. As we have shown, this approach performs practically identical to XBSsX, which is a more accurate variant than RPAsX (the method advocated originally by Maggio and Kresse⁸). There is an important difference, though. In the present work, the polarization propagators are evaluated using Kohn–Sham orbital energies. This approximation was not investigated by Maggio and Kresse for the homogeneous electron gas, since it tends to overestimate the absolute correlation energy (which is also the case for atoms, as demonstrated in Table II).

TABLE V. Errors in the harmonic vibrational frequencies (ω_e in cm^{-1}) of transition-metal monoxides. Computed in the def2-QZVP basis set. Hartree-Fock reference for UHF-CCSD(T), TPSS reference elsewhere.

Method	CaO	ScO	TiO	VO	CrO	MnO	FeO	CoO	NiO	CuO	ZnO	MAE ^a
Expt. ^b	732	965	1009	1011	898	840	880	853	838	640	727 ^c	
CCSD(T) ^d	-33	-16	39	-83	16	14	67	145	132	-28	19	54
TPSS	43	9	6	4	15	67	43	8	15	25	36	25
TPSS orbital energies												
dRPA ^e	-37	-66	-65	-46	-36	-51	23	25	43	28	49	43
AXK ^e	-12	-24	-10	18	5	39	39	71	58	-48	-43	33
CC-SOSEX	54	30	51	89	81	84	111	217	212	-123	15	97
AC-SOSEX	56	32	54	95	93	88	116	230	222	-136	12	103
dRPA-II	-42	-87	-54	-12	120	33	-1	-60	32	-80	...	52
dRPA-II _s X	120	89	119	167	165	137	186	376	367	-169	81	180
RPA _s X''	-59	-83	-73	-62	-18	15	-16	-61	-64	12	-72	49
XBS _s X''	-54	-75	-65	-53	-15	15	-12	-60	-58	3	-71	44
CC-IOSEX''	-61	-84	-74	-63	-17	13	-18	-65	-70	10	-75	50
IOSEX _s X''	-55	-76	-65	-52	-15	14	-12	-53	-56	-2	-74	43
evGW quasiparticle energies												
RPA _s X	-12	-19	3	36	-63	57	30	-201	174	24	102	66
RPA _s X'	-32	-55	-46	-29	-2	40	31	13	15	10	-18	27
XBS _s X	-11	-17	1	44	-56	70	43	-67	129	-25	95	51
XBS _s X'	-20	-41	-29	-10	12	45	43	43	53	-9	-7	28
CC-IOSEX	-11	-18	5	37	-62	56	29	-202	173	13	102	64
CC-IOSEX'	-33	-55	-47	-29	0	40	29	13	12	6	-17	26
IOSEX _s X'	-14	-34	-24	-3	19	49	50	60	74	-18	15	33

a) Mean absolute error.

b) For details on experimental data, cf. Ref. 41.

c) CCSD(T) result from Ref. 43.

d) Frozen-core (M: $1s2s2p$, O: $1s$) UHF-CCSD(T)/def2-QZVPP computation with CFOUR.

e) Computed with the RIRPA module.

f) Computation failed.

Absolute errors in the correlation energy are, however, often acceptable: for the homogeneous electron gas, the most relevant property is that the density dependence of the correlation energy is well reproduced, a constant offset hardly matters.

Priority Programme 1807 (Control of London Dispersion Interactions in Molecular Chemistry). X.G. gratefully acknowledges financial support by the DFG through the Transregional Collaborative Research Centre 88 [Cooperative Effects in Homo- and Heterometallic Complexes (3MET)].

ACKNOWLEDGMENTS

C.H. gratefully acknowledges financial support by the Deutsche Forschungsgemeinschaft (DFG) through the

¹ S. Albrecht, L. Reining, R. Del Sole, and G. Onida, Phys. Rev. Lett. **80**, 4510 (1998).

² E. K. Chang, M. Rohlfing, and S. G. Louie, Phys. Rev. Lett. **85**, 2613 (2000).

³ X. Blase, I. Duchemin, and D. Jacquemin, Chem. Soc. Rev. **47**, 1022 (2018).

⁴ F. Furche, R. Ahlrichs, C. Hättig, W. Klopper, M. Sierka, and F. Weigend, WIREs: Comput. Mol. Sci. **4**, 91 (2014).

- TURBOMOLE V7.2 2017, a development of University of Karlsruhe and Forschungszentrum Karlsruhe GmbH, 1989-2007; TURBOMOLE GmbH, since 2007; available from <http://www.turbomole.com>.
- ⁶ K. Krause and W. Klopper, *J. Comput. Chem.* **38**, 383 (2017).
 - ⁷ X. Gui, C. Holzer, and W. Klopper, *J. Chem. Theory Comput.* **14**, 2127 (2018).
 - ⁸ E. Maggio and G. Kresse, *Phys. Rev. B* **93**, 235113 (2016).
 - ⁹ K. Pernal, *Int. J. Quantum Chem.* **118**, e25462 (2018).
 - ¹⁰ G. P. Chen, V. K. Voora, M. M. Agee, S. G. Balasubramani, and F. Furche, *Ann. Rev. Phys. Chem.* **68**, 421 (2017).
 - ¹¹ H. Eshuis, J. E. Bates, and F. Furche, *Theor. Chem. Acc.* **131**, 1084 (2012).
 - ¹² X. Ren, P. Rinke, C. Joas, and M. Scheffler, *J. Mater. Sci.* **47**, 7447 (2012).
 - ¹³ A. Hefelmann and A. Görling, *Mol. Phys.* **109**, 2473 (2011).
 - ¹⁴ J. G. Ángyán, R.-F. Liu, J. Toulouse, and G. Jansen, *J. Chem. Theory Comput.* **7**, 3116 (2011).
 - ¹⁵ W. Klopper, A. M. Teale, S. Coriani, T. B. Pedersen, and T. Helgaker, *Chem. Phys. Lett.* **510**, 147 (2011).
 - ¹⁶ M. E. Harding, J. Vázquez, B. Ruscic, A. K. Wilson, J. Gauss, and J. F. Stanton, *J. Chem. Phys.* **128**, 114111 (2008).
 - ¹⁷ G. Jansen, R.-F. Liu, and J. G. Ángyán, *J. Chem. Phys.* **133**, 154106 (2010).
 - ¹⁸ K. Krause and W. Klopper, *J. Chem. Phys.* **139**, 191102 (2013).
 - ¹⁹ W. Zhu, L. Zhang, and S. B. Trickey, *J. Chem. Phys.* **145**, 224106 (2016).
 - ²⁰ J. Toulouse, I. C. Gerber, G. Jansen, A. Savin, and J. G. Ángyán, *Phys. Rev. Lett.* **102**, 096404 (2009).
 - ²¹ J. Toulouse, W. Zhu, J. G. Ángyán, and A. Savin, *Phys. Rev. A* **82**, 032502 (2010).
 - ²² A. Grüneis, M. Marsman, J. Harl, L. Schimka, and G. Kresse, *J. Chem. Phys.* **131**, 154115 (2009).
 - ²³ X. Ren, A. Tkatchenko, P. Rinke, and M. Scheffler, *Phys. Rev. Lett.* **106**, 153003 (2011).
 - ²⁴ M. Shishkin, M. Marsman, and G. Kresse, *Phys. Rev. Lett.* **99**, 246403 (2007).
 - ²⁵ CFOUR, a quantum chemical program package written by J. F. Stanton, J. Gauss, L. Cheng, M. E. Harding, D. A. Matthews, P. G. Szalay, with contributions from A. A. Auer, R. J. Bartlett, U. Benedikt, C. Berger, D. E. Bernholdt, Y. J. Bomble, O. Christiansen, F. Engel, R. Faber, M. Heckert, O. Heun, M. Hilgenberg, C. Huber, T.-C. Jagau, D. Jonsson, J. Jusélius, T. Kirsch, K. Klein, W. J. Lauderdale, F. Lipparini, T. Metzroth, L. A. Mück, D. P. O'Neill, D. R. Price, E. Prochnow, C. Puzzarini, K. Ruud, F. Schiffmann, W. Schwalbach, C. Simmons, S. Stopkowicz, A. Tajti, J. Vázquez, F. Wang, J. D. Watts, and from the integral packages MOLECULE (J. Almlöf and P. R. Taylor), PROPS (P. R. Taylor), ABACUS (T. Helgaker, H. J. Aa. Jensen, P. Jørgensen, and J. Olsen), and with ECP routines by A. V. Mitin and C. van Wüllen. For the current version, see <http://www.cfour.de>.
 - ²⁶ K. Raghavachari, G. W. Trucks, J. A. Pople, and M. Head-Gordon, *Chem. Phys. Lett.* **157**, 479 (1989).
 - ²⁷ J. D. Watts, J. Gauss, and R. J. Bartlett, *J. Chem. Phys.* **98**, 8718 (1993).
 - ²⁸ K. A. Peterson and T. H. Dunning Jr., *J. Chem. Phys.* **117**, 10548 (2002).
 - ²⁹ R. A. Kendall, T. H. Dunning Jr., and R. J. Harrison, *J. Chem. Phys.* **96**, 6796 (1992).
 - ³⁰ B. P. Prascher, D. E. Woon, K. A. Peterson, T. H. Dunning Jr., and A. K. Wilson, *Theor. Chem. Acc.* **128**, 69 (2011).
 - ³¹ C. Hättig, *Phys. Chem. Chem. Phys.* **7**, 59 (2005).
 - ³² F. Weigend, *Phys. Chem. Chem. Phys.* **8**, 1057 (2006).
 - ³³ T. Helgaker, W. Klopper, H. Koch, and J. Noga, *J. Chem. Phys.* **106**, 9639 (1997).
 - ³⁴ A. Halkier, T. Helgaker, P. Jørgensen, W. Klopper, and J. Olsen, *Chem. Phys. Lett.* **302**, 437 (1999).
 - ³⁵ X. Blase, C. Attaccalite, and V. Olevano, *Phys. Rev. B* **83**, 115103 (2011).
 - ³⁶ J. Tao, J. P. Perdew, V. N. Staroverov, and G. E. Scuseria, *Phys. Rev. Lett.* **91**, 146401 (2003).
 - ³⁷ V. N. Staroverov, G. E. Scuseria, J. Tao, and J. P. Perdew, *J. Chem. Phys.* **119**, 12129 (2003).
 - ³⁸ V. N. Staroverov, G. E. Scuseria, J. Tao, and J. P. Perdew, *J. Chem. Phys.* **121**, 11507 (2004).
 - ³⁹ J. E. Bates and F. Furche, *J. Chem. Phys.* **139**, 171103 (2013).
 - ⁴⁰ F. Weigend, F. Furche, and R. Ahlrichs, *J. Chem. Phys.* **119**, 12753 (2003).
 - ⁴¹ F. Furche and J. P. Perdew, *J. Chem. Phys.* **124**, 044103 (2006).
 - ⁴² E. R. Davidson, S. A. Hagstrom, S. J. Chakravorty, V. M. Umar, and C. F. Fischer, *Phys. Rev. A* **44**, 7071 (1991).
 - ⁴³ C. W. Bauschlicher Jr. and H. Partridge, *J. Chem. Phys.* **109**, 8430 (1998).

